JOC The Journal of Organic Chemistry

Article

pubs.acs.org/joc

Mechanism of the Intramolecular Hexadehydro-Diels–Alder Reaction

Daniel J. Marell,[‡,§] Lawrence R. Furan,[†,§] Brian P. Woods,[‡] Xiangyun Lei,[‡] Andrew J. Bendelsmith,[†] Christopher J. Cramer,[*,‡] Thomas R. Hoye,[*,‡] and Keith T. Kuwata[*,†]

[†]Department of Chemistry, Macalester College, Saint Paul, Minnesota 55105-1899, United States

[‡]Department of Chemistry, Supercomputing Institute, and Chemical Theory Center, University of Minnesota, Minneapolis, Minnesota 55455-0431, United States

Supporting Information

ABSTRACT: Theoretical analysis of the mechanism of the intramolecular hexadehydro-Diels–Alder (HDDA) reaction, validated against prior and newly measured kinetic data for a number of different tethered yne-diynes, indicates that the reaction proceeds in a highly asynchronous fashion. The rate-determining step is bond formation at the alkyne termini nearest the tether, which involves a transition-state structure exhibiting substantial diradical character. Whether the reaction then continues to close the remaining bond in a concerted fashion or in a stepwise fashion (i.e., with an intervening intermediate) depends on the substituents at the remaining terminal alkyne positions. Computational modeling of the HDDA reaction is complicated by the significant diradical character that arises along the reaction coordinate, which leads to instabilities in both restricted singlet Kohn–Sham density functional theory (DFT) and coupled cluster theory based on a Hartree–Fock reference wave function. A consistent picture emerges, however, from comparison of broken-symmetry DFT calculations and second-order perturbation theory based on complete-active-space self-consistent-field (CASPT2) calculations.

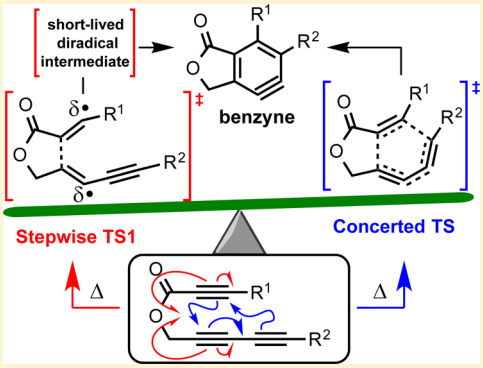

INTRODUCTION

The hexadehydro-Diels–Alder (HDDA) cascade (Figure 1a) involves an initial rate-limiting, thermal cycloisomerization of a triyne to a benzyne intermediate[1−3] followed by a trapping reaction. The overall process has been shown to be quite general[4] and serves as a platform for the discovery of new reaction processes.[5,6] Coupled cluster calculations including single, double, and perturbatively estimated triple excitations (CCSD(T)) indicate that *o*-benzyne is approximately 50 kcal/mol more stable than 1,3-butadiyne and ethyne.[7] Similar exergonicities have been computed for the free energy changes that attend intramolecular HDDA processes.[4] Like the classic Diels–Alder reaction between a diene and dienophile, for which extensive mechanistic interrogation has been undertaken, the HDDA could potentially proceed through one of two pathways (Figure 1b). In a concerted process (magenta arrows) the a–b and c–d bonds form simultaneously, which is to say that no intermediate intervenes prior to product formation, irrespective of the degree of synchronicity in the formation of the two bonds. Alternatively, in a stepwise pathway, the proximal bond a–b is formed first (blue arrows) to create a diradical intermediate, which then ring-closes by formation of the distal bond c–d (green arrows); bond formation in the reverse order (c-to-d then a-to-b) is formally plausible, but clearly unlikely (*vide infra*). At the coupled cluster level of theory, the concerted and stepwise pathways for the parent HDDA reaction between ethyne and butadiyne are predicted to have activation barriers within 0.5 kcal/mol of one another;[7] however, as discussed in this paper, there is reason to believe that this level of theory may underestimate the stability of diradical transition-state (TS) structures. Houk and co-workers have recently reported broken-symmetry density-functional theory (DFT) studies for a hypothetical series of bimolecular HDDA reactions between 1,3-butadiyne and four different diynophiles.[8] In each case, including the parent reaction, they identified a preference for a stepwise, diradical pathway over the concerted event. They found in addition that the barriers for ring closure of the generated diradical intermediate, to complete the generation of the *o*-benzyne species, were quite low (in the range of 4–7 kcal/mol). Larini, Perrin, and coworkers have recently reported a DFT examination of an intramolecular HDDA reaction (of a tetrayne substrate) in which they also observed a preference for a stepwise, diradical pathway.[9]

To gain further mechanistic insight into the details of HDDA cycloisomerizations, which to date have only been observed in intramolecular settings, we have carried out additional experimental and computational studies reported here. In particular, the energies of activation of a new series of six triyne substrates have been determined experimentally and evaluated computationally using a variety of DFT and wave function

Special Issue: 50 Years and Counting: The Woodward-Hoffmann Rules in the 21st Century

Received: June 15, 2015
Published: August 13, 2015

DOI: 10.1021/acs.joc.5b01356
J. Org. Chem. 2015, 80, 11744–11754

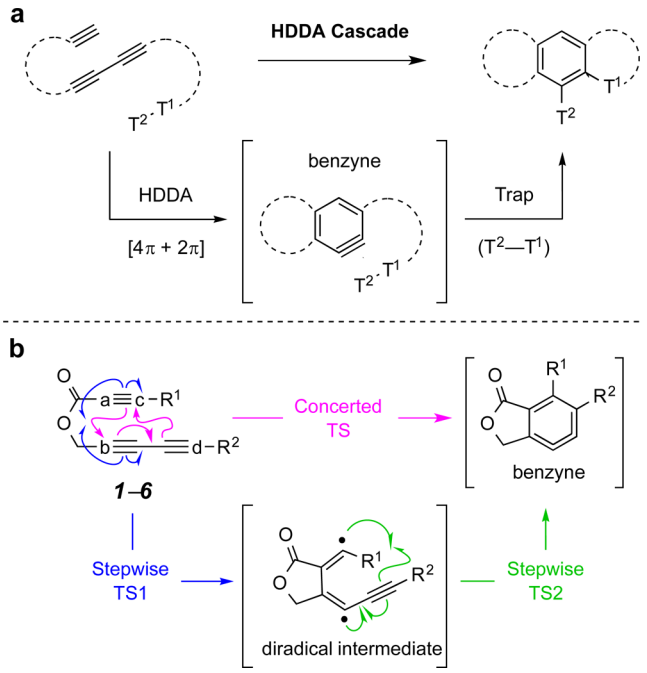

Figure 1. (a) Intramolecular hexadehydro-Diels–Alder (HDDA) reaction of a generic tethered triyne substrate, followed by intramolecular trapping. (b) Concerted vs stepwise mechanistic alternatives. See Table 1 for substituents defining for **1–6**.

theory methods. On this specific test set we address the questions of (i) is the HDDA reaction better described as a concerted or a stepwise diradical pathway? and (ii) to what degree does diradical character along the stepwise reaction pathway affect the applicability of theoretical methods based on single-determinantal references? We then extend our theoretical attention to additional HDDA substrates for which kinetic data are available and show that broken-symmetry DFT calculations agree with multireference wave function theory calculations. This helps in distinguishing between a reaction pathway that is fully stepwise vs one that is concerted but so asynchronous as to be effectively stepwise, albeit with an intermediate on the potential energy surface that is not predicted to have a bound vibrational state.

RESULTS AND DISCUSSION

Theory/Computational Models. Gas-phase molecular structures were fully optimized at the M06-2X level[10] of density functional theory employing the 6-311+G(d,p) basis set.[11] This level of theory has been documented to give very good agreement with experiment for organic structures.[12] The natures of all stationary points, either minima or TS structures, were confirmed by analytic computation of vibrational frequencies, which were also employed for the calculation of molecular partition functions and thermal contributions to molecular enthalpies and free energies.

"Best" DFT electronic energies were computed using the B3LYP functional[13] combined with the 6-311+G(d,p) basis set and a D3 dispersion correction[14] damped according to the scheme of Becke and Johnson.[15] In addition, *o*-dichlorobenzene solvation effects were included in these single-point calculations using the SMD solvation model.[16] This level of theory, denoted in full as SMD(*o*-dichlorobenzene)/B3LYP-D3BJ/6-311+G(d,p)//M06-2X/6-311+G(d,p), will be referred to simply as B3LYP-D3BJ hereafter. In select instances, geometries and energetics were also computed using other levels of density functional theory, including M06-L, M06, M06-D3, M06-2X, M11-L, M11, and B3LYP; full details are provided either below or in the Supporting Information (SI).

Importantly, while restricted Kohn–Sham determinants for relevant singlet electronic (ground) states were found to be stable to symmetry breaking for all reactants, this was *not* the case for any of the concerted TS structures that were located. Unrestricted (broken-symmetry) determinants were optimized for TS structures, and intermediates along stepwise cyclization pathways and singlet energies ^1E were determined from spin purification of the mixed-spin-state energies according to refs 17 and 18 where the "BS" and "3" superscripts in eq 1 refer to broken-symmetry and triplet Kohn–Sham determinants, respectively, and $\langle S^2\rangle$ is the expectation value of the total spin operator.

$$^1E = \frac{2\cdot{}^{BS}E - {}^{BS}\langle S^2\rangle\cdot{}^3E}{2 - {}^{BS}\langle S^2\rangle} \quad (1)$$

To address the instability of the restricted Kohn–Sham determinants, we also applied, in select cases, second-order perturbation theory based on complete-active-space self-consistent-field (CASPT2) calculations,[19] taking for the active space the 12 electrons in 12 orbitals associated with the π and π^* orbitals for the three triple bonds and using the triple-ζ ANO-RCC basis set of Roos et al.[20] An IPEA shift of 0.25 au (the default value) was applied in the CASPT2 calculations to define the zeroth-order Hamiltonian.[21] We also examined the CBS-QB3 level of theory[22] in certain instances. This composite electronic structure method assembles molecular energies from a variety of levels with the most complete being coupled cluster theory including single, double, and perturbatively estimated triple excitations (CCSD(T)); for singlets, however, the default CBS-QB3 procedure is based on a single-determinant reference RHF wave function, and we computed the T1 diagnostic[23] of Lee and Taylor to assess the degree to which this might render the CBS-QB3 level unreliable. In order to apply CBS-QB3 to diradical species, we calculated each of the contributing molecular energies based on a broken-symmetry Hartree–Fock reference.

Density functional enthalpies and free energies were computed from Boltzmann averages over all relevant structures[18] (note that solvation free energies from continuum solvent calculations are *not* readily separable into enthalpies and entropies, but because we are interested only in *relative* enthalpies, the assumption that any variation in the solvation enthalpies is similar to that in the solvation free energies seems reasonable, given the overall structurally similar nature of the substrates). Averaging was required only for reactant minima having free rotation about single bonds in the tether joining the reactive 4π and 2π fragments. For these substrates, rotamers placing the triple bonds into proximity with one another (i.e., in a "pre-reactive" conformation) were invariably higher than alternatives with the reactive fragments oriented away from one another. Other averages (e.g., rotameric populations associated with a TBS group) were assumed to cancel in reactant and TS structures.

Mechanistic Analysis. At the outset, our thinking was influenced by extensive qualitative observations some of us have made about many HDDA reaction cascades. For example, they are essentially insensitive to the presence or absence of triplet oxygen, light, or good hydrogen-atom donor solvents such as

DOI: 10.1021/acs.joc.5b01356
J. Org. Chem. 2015, 80, 11744–11754

chloroform, observations more compatible with the hypothesis of a concerted reaction mechanism. We therefore designed and prepared a series of substrates to test this possibility. Esters **1**–**6** (Figure 1 and Table 1) differ substantially in the steric bulk of

Table 1. Half-Lives (h) and Relative Rates for HDDA Cyclization of Ester Triynes 1–6

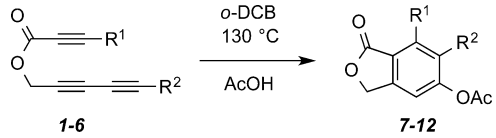

1-6 *7-12*

triyne substrate	R^1	R^2	$t_{1/2}$, h	k_{rel}	phthalide product
1	H	H	4.5	1.1	**7**
2	H	TMS	2.8	1.8	**8**
3	H	TBS	2.8	1.8	**9**
4	H	$SiPh_3$	2.8	1.8	**10**
5	TMS	H	1.1	4.5	**11**
6	TMS	TMS	5.0	1.0	**12**

the trisubstituted silyl substituents on one or both of their terminal alkynes. We presumed that enhanced bulk would slow the rate of HDDA cyclization, if concerted. The preparation of esters **1**–**6** was straightforward. Each ester was heated in 1,2-dichlorobenzene (*o*-DCB) in the presence of 20–40 equiv of acetic acid, a known and efficient trap of HDDA-generated benzynes. Half-lives were measured by following the conversion to product at various time points via ^{1}H NMR spectroscopy. Surprisingly, all six substrates exhibited reaction rates within a factor of 4.5 of one another, and the least and most highly substituted variants (i.e., **1** and **6** respectively) cyclized at essentially the same rate (k_{rel} of 1.1). This observation is more consistent with the reaction proceeding through a rate-limiting transition state in which the distal alkyne termini are quite far from one another. Such a situation can be envisioned for *either* a highly asynchronous concerted process or a stepwise diradical pathway (Figure 1b).

We then turned to computational modeling. For each of the educts **1**–**6**, we located multiple conformational minima related as rotamers. In general, "unreactive" conformers (e.g., the *anti* conformer shown at left in Figure 2) predominated; specifically, the percentages of *syn*-like "reactive" conformers at the B3LYP-D3BJ//M06-2X level were predicted to be 3, 3, 14, 3, 11, and

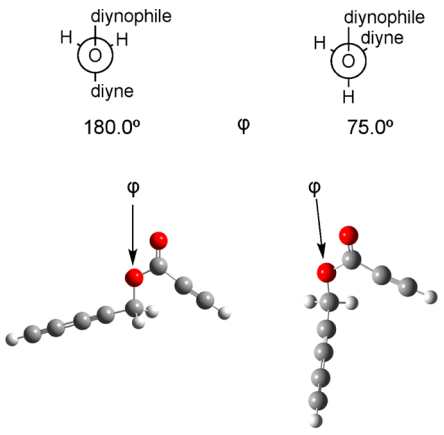

Figure 2. Fischer projections and ball-and-stick models of two rotameric minima for **1**.

28 for **1**–**6**, respectively. Proper enthalpies of reaction must take into account Boltzmann averages over all contributors to the educt population, and this was indeed done as noted in the Theory/Computational Models Section.

With respect to transition states for a concerted reaction, for substrates **1**–**5** it proved possible to locate TS structures on the singlet surface using a restricted Kohn–Sham formalism (in the case of **6**, such a TS structure could not be located, presumably owing to instability of the restricted determinant, as discussed in more detail below). Perturbing these structures in either direction along the reaction coordinate led either back to educts or forward to *o*-benzyne products; i.e., they are TS structures for concerted HDDA cycloaddition. Consistent with concerted reactivity, the lengths of the two newly forming bonds connecting the termini of the former yne and diyne fragments were reasonably similar, e.g., in the case of **1**, 2.018 Å for the forming bond nearer the ester tether and 2.463 Å for the other (cf. the length difference of ca. 3 Å for the stepwise pathway, below). Comparison (Table 2) of the computed activation

Table 2. Experimentally Derived and Predicted Concerted and Stepwise Activation Enthalpies (kcal/mol) for 1–6

		$\Delta H^{\ddagger}$			
			Theoretical[a]		
	Triyne	Experiment[b]	Concerted TS	Stepwise TS1	Stepwise TS2[c]
1	H/H	23.7	31.5	25.5	18.1 (−0.8)
2	H/TMS	23.3	30.4	24.8	16.5 (−1.2)
3	H/TBS	23.3	30.3	24.8	16.4 (−1.3)
4	H/$SiPh_3$	23.3	28.8	24.6	*d*
5	TMS/H	22.5	28.9	23.1	17.1 (0.2)
6	TMS/TMS	23.8	*d*	20.9	18.8 (4.8)

[a]Relative to the Boltzmann-averaged enthalpy of the educt. [b]Determined from relative rates and assuming a common Arrhenius *A* value; see Experimental Section for details. [c]Enthalpy in parentheses is relative to the diradical intermediate; a negative value implies an enthalpy *below* that of the intermediate, in spite of a higher potential energy. [d]Not located.

enthalpies to those derived from experiment, however, does not give a particularly close match for **1**–**5**. The computed values are all substantially higher than the experimental ones, and the computed values range over 2.7 kcal/mol while the experimental values range over only 1.3 kcal/mol.

Further assessment of the Kohn–Sham determinants for the concerted TS structures revealed them to be unstable to spin-symmetry breaking (i.e., they exhibited a restricted → unrestricted determinantal instability). Reoptimization using a broken-symmetry unrestricted Kohn–Sham formalism led in every case to a *new* TS structure in which bond formation between the alkyne termini connected proximally to the tether was evident, but the remaining distal alkyne termini remained far apart. In the case of **1**, for instance, the forming C–C bond length in this broken-symmetry TS structure is 1.779 Å, while the distance between the remaining alkyne termini is 4.740 Å. These TS structures, then, are consistent with *stepwise* reactivity. In the case of **6**, it was possible to locate this stepwise TS structure even though it had not proven possible to find a concerted TS structure. In every instance where a comparison could be made, these stepwise TS structures were predicted to be 4–6 kcal/mol lower in energy than the corresponding concerted TS structures. The broken-symmetry

DOI: 10.1021/acs.joc.5b01356
J. Org. Chem. 2015, 80, 11744–11754

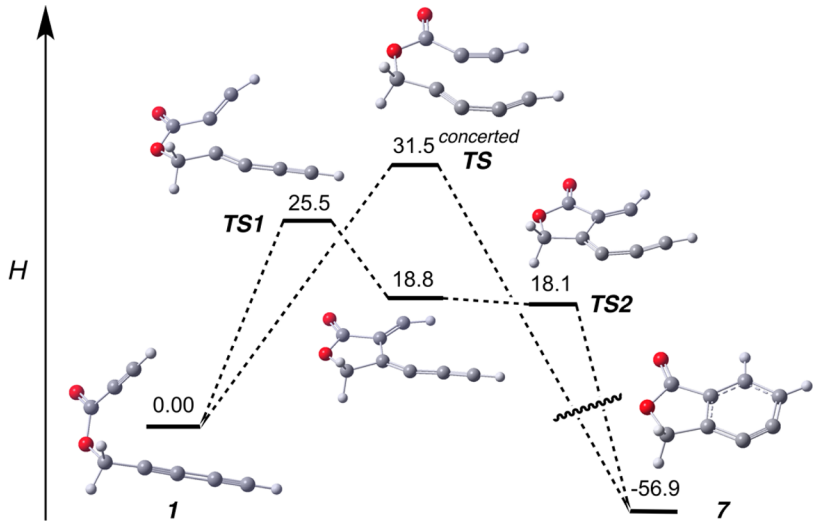

Figure 3. Concerted and stepwise-like reaction paths for **1** at the B3LYP-D3BJ level of theory; relative enthalpies are reported in kcal/mol from the B3LYP-D3BJ level (individual structures are shown, but relative enthalpies are computed from a Boltzmann average over all relevant contributors).

TS structures were all characterized by $\langle S^2 \rangle$ values of ~0.45, consistent with significant diradical character.

As expected for a stepwise pathway, in each case except for **4** it was also possible using broken-symmetry Unrestricted Density Functional Theory (UDFT) to locate diradical intermediates (having $\langle S^2 \rangle$ values very near 1.00) and in addition subsequent TS structures for the formation of the second C−C bond leading to *o*-benzyne products. We will distinguish these two TS structures along any stepwise path as TS1 and TS2 for purposes of discussion. Enthalpies computed for TS2 structures were in every case below those computed for TS1; i.e., it is TS1 that is predicted to be rate determining. Interestingly, while intermediate diradicals between these two TS structures could be identified on the potential energy surface in every case other than **4**, including zero-point vibrational energies and 298 K enthalpic contributions caused the enthalpy of TS2 to fall below that of the intermediate in several instances. The reaction in such cases is stepwise on the potential energy surface, but from an enthalpic standpoint may be viewed as concerted, albeit extremely asynchronous—consistent with the term "stepwise-like," if we indulge in such coinage of a term. For **4**, on the other hand, it was not possible to find an intermediate diradical, so the reaction truly is predicted to be concerted, even with broken-symmetry DFT, but it is extremely asynchronous.

If we now consider the predicted energetics associated with the rate-determining TS1 structures (Table 2), we see that, for **1**−**5**, theory overestimates the enthalpy of activation in every case, but by an average of only 1.3 kcal/mol. The variation across all five substrates is 2.4 kcal/mol, which is still larger than that observed in the experimental data, although by a slightly smaller margin than predicted for the concerted reaction paths. These results taken as a whole argue for assignment of the mechanism of the intramolecular HDDA reaction as stepwise(-like). For the case of **1**, the various reaction paths are compared to one another in Figure 3.

Given the reasonably good correlation of computed and experimental values for the others, it is somewhat surprising that B3LYP-D3BJ predicts a substantially smaller activation enthalpy for the bis-trimethylsilylated substrate **6** than is observed experimentally. Such a prediction is consistent with an enhanced stability of the diradical intermediate that is produced, as might be expected given silyl substitution at both radical centers (such stability is also manifest in the higher barrier remaining for completion of this cycloaddition compared to substrates **1**−**5**).[24] Nevertheless, repeat experiments confirmed that **1** and **6** cyclize with very similar rates. We considered whether the assumption of common Arrhenius *A* values might be invalid in this instance, but inspection of computed entropies of activation (a simple relationship exists between the entropy of activation and the Arrhenius *A* value[18]) suggested that any difference would be unlikely to account for more than a few tenths of a kcal/mol variation in the activation enthalpy. Another possibility is some specific interaction with the surrounding solvent that is unique to the doubly silyl-substituted **6**, but we did not explore this further.

Instead, we chose to expand our consideration to an additional six substrates for the intramolecular HDDA reaction (top of Table 3) for which experimental kinetic data are also available.[25] A comparison of activation enthalpies continuing to employ the B3LYP-D3BJ level of theory is presented in Table 3, focusing exclusively on the stepwise(-like) reaction coordinate. It is apparent that there is *very* good agreement between theory and experiment, with the error being less than 1.1 kcal/mol in every case except for **14**, where the error is 3.0 kcal/mol. However, the "experimental" value of the Arrhenius activation energy (which is used to determine the activation enthalpy: $E_a = \Delta H^{\ddagger} + RT$[18]) is likely *under*estimated in the case of **14** because it was determined from the observed rate by assuming the same *A* value that is used for compounds having free rotation about all single bonds in the tether. The use of the alternative and larger *A* value that is determined/employed for compounds having far less rotational freedom (i.e., **13**, **16**, and **18**; see Experimental Section) would increase the experimental enthalpy of activation reported in Table 3 by nearly 2 kcal/mol and bring it into much closer agreement with theory. The actual *A* value for **14**, which has moderately restricted rotation, is likely somewhere in between the two extreme values, but temperature-dependent measurements have not been made to assess this point more quantitatively. In any case, the mean signed and unsigned errors comparing theory and experiment for **13**−**18** provide additional strong support for the assignment

DOI: 10.1021/acs.joc.5b01356
J. Org. Chem. 2015, 80, 11744−11754

Table 3. Experimentally Derived and Computed Activation Enthalpies (kcal/mol) for 13−18

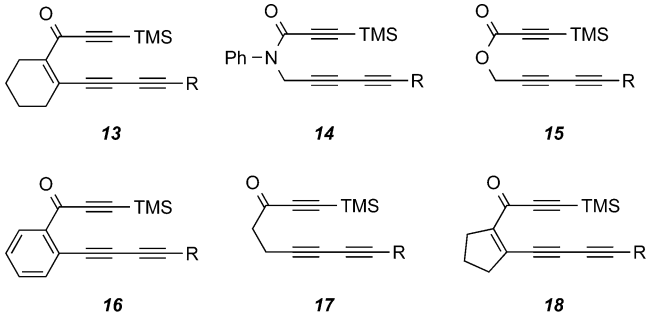

$R_{experimental}$ = $(CH_2)_2OTBS$ $R_{computed}$ = Et

	$\Delta H^{\ddagger}$	
Compound	Experimental	B3LYP-D3BJ TS1
13	19.1	19.1
14	21.4	24.4
15	22.6	23.5
16	22.7	21.6
17	27.0	27.4
18	27.2	26.7
MSE[a]		0.45
MUE[b]		0.98

[a]Mean signed error. [b]Mean unsigned error.

of a stepwise(-like) mechanism to the intramolecular HDDA reaction.

We close this subsection by noting the degree to which theory provides an important rationalization for two seemingly inconsistent experimental observations, namely (i) rates that appear largely insensitive to steric bulk at the distal termini of the reacting alkyne linkages, and thus seem more in support of a stepwise mechanism, and (ii) the failure of external additives (solvent, oxygen, or phenolic radical inhibitors) to alter the course of reaction, expected for pathways involving intermediates having (di)radical character, which supports a concerted mechanism. In this instance, the reaction appears to be balanced on the knife edge between these two formal pathways. Thus, there is a rate-determining TS structure that has essentially no bond formation occurring at the distal termini, but the resulting intermediate diradical either fails to be a minimum or, if it is a minimum, fails to have a sufficient lifetime to be trapped prior to crossing a second transition state to complete the cycloaromatization. Indeed, insofar as the potential energy surfaces for the reactions studied here represent 0 K Born−Oppenheimer topologies that are relatively flat, at more typical reaction temperatures one would expect reactive trajectories to sample a broad range of structures, with some trending toward more concerted, albeit still quite asynchronous, overall reaction paths.

One may regard the intramolecular HDDA in some respects as a variation on the known dimerization reaction of alkynes to generate 1,3-butadiene-diyl intermediates,[26] a process that Haberhauer and Gleiter have recently predicted to be competitive with Bergman cyclization when sufficiently high concentrations of substrate outweigh the otherwise entropically favored intramolecular process.[27] A key difference in the two processes, however, is that the diradical intermediate that is formed in the alkyne dimerization process is preferentially *s*-trans in geometry, and immediate closure to a formal [2 + 2] cycloadduct is expected to be kinetically disfavored, compared to other radical reactions, given the very high strain energy associated with the product cyclobutadiene ring. In the HDDA example, by contrast, the developing radical character of one of the vinyl centers is progressively delocalized in an "in-plane" allylic sense to the remaining alkyne terminus, which creates an opportunity for ring closure to the six-membered benzyne, a more energetically favorable option. Indeed, in the intramolecular case with a reasonably short tether, the geometry lending itself to such an outcome is essentially so constrained. As noted in the introduction, Houk and co-workers[8] have found diradical pathways to be operative in their theoretical studies of *inter*molecular HDDA reactions, and it would not be surprising if experiment were to reveal such reactions to generate longer-lived diradical intermediates (the promiscuity of which might compromise the reaction's synthetic utility)—to date, however, no experimental results are available against which to assess this point. It is also relevant that small, unsubstituted conjugated poly-ynes such as 1,3-butadiyne[28a] and 1,3,5-hexatriyne[28b] (a natural product!) are known to detonate when handled as neat substances.

The intramolecular HDDA reaction is in some sense unique among hydrocarbon cycloaromatization reactions, insofar as the diradical character generated along the reaction coordinate is predisposed to continue reaction so as readily to join what would otherwise be two radical centers into a new bond (noting that the so-produced *o*-benzyne cycloadduct *does* have some biradical character,[29] but *o*-benzynes are nevertheless generally regarded as highly reactive closed-shell species in organic synthesis[30]). This is in contrast, then, to the Bergman cycloaromatization of an enediyne,[31] which generates a diradical *p*-benzyne intermediate that is incapable of further closure owing to the instability of what would be a "Dewar benzyne" product.[32] The intramolecular HDDA is also in contrast with the Myers−Saito[33] and Schmittel[34] cycloaromatizations of enyne-allenes, which lead to α,3-didehydrotoluene and extracyclic fulvenoid diradical intermediates, respectively,[32e,35] and with the cycloaromatization of the enyne-cumulene neocarzinostatin chromophore, which leads to a 1,5-didehydroindene.[36] In none of these other cases are the radical centers able to react (intramolecularly) with one another to form a new bond (and ring): geometric constraints prevent such a closure.

While the particular circumstances of the intramolecular HDDA make it possible for an intermediate with diradical character to close productively, one may certainly ask the question, why is there diradical character at all? Why does the reaction not occur in a fully concerted fashion? It is not obvious that there is an intuitively simple answer to this question, and indeed our calculations predict that the degree of diradical character is quite sensitive to substitution (cf. Table 2), suggesting that a continuum of reactivity may be accessed based on steric and electronic factors that differentially affect alternative transition-state structures. At one time, a lively debate centered on the propensity of electrocyclic reactions to undergo concerted vs stepwise reaction mechanisms.[37] The intramolecular HDDA reaction is an interesting new contributor to this discussion, to the extent that in its case the answer seems to be, "It depends."

While experiments examining kinetic isotope effects (KIEs) for intramolecular HDDA reactions have yet to be performed, we have carried out calculations for **1** that indicate that they may be expected to be potentially useful for further

DOI: 10.1021/acs.joc.5b01356
J. Org. Chem. 2015, 80, 11744−11754

distinguishing between stepwise-like and fully concerted reactivity (Table 4). In particular, compared to the concerted TS structure, in the stepwise-like TS structure the more significant rehybridizations of the distal termini associated with developing radical character lead to noteworthy predicted differences in secondary H/D KIEs. In addition, the *difference* in the secondary $^{12}C/^{13}C$ KIEs for the proximal vs the distal alkyne termini is predicted to be considerably larger for the stepwise-like TS structure than for the concerted structure (KIEs for the interior carbon atoms in the diyne fragment do not show much sensitivity to TS structure and are unlikely to be useful for distinguishing between the two mechanisms).

Table 4. Secondary Kinetic Isotope Effects (Dimensionless) Predicted at the B3LYP-D3BJ Level for the Parent Triyne 1

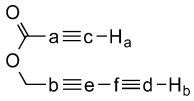

Position	Concerted TS	Stepwise TS1
C_a	1.0220	1.0398
C_b	1.0211	1.0360
C_c	1.0202	1.0158
C_d	1.0138	1.0040
C_e	1.0098	1.0160
C_f	1.0072	1.0080
H_a	1.0569	1.0863
H_b	1.0028	1.0237

Additional Computational Analysis. This section provides additional support for the mechanistic analysis provided above, but is likely to be of interest primarily to specialists, as it addresses technical details associated with further validation of the computations beyond simple comparison to experimental quantities. Such a comparison is especially important because the structures and energies computed from DFT prove to be extraordinarily sensitive to the choice of functional, which can certainly lead to decreased confidence in interpretation, even when good quantitative agreement with measured quantities appears to be achieved by a particular functional choice. In such situations, it is helpful to employ alternative levels of electronic structure theory, the design of which may render them less sensitive than DFT to particular challenges.

To begin, we note that activation enthalpies predicted for the concerted or stepwise TS structures, from restricted and unrestricted single-point calculations with other functionals, respectively, span a very wide range. Of the functionals tested, the smallest and largest enthalpies of activation associated with

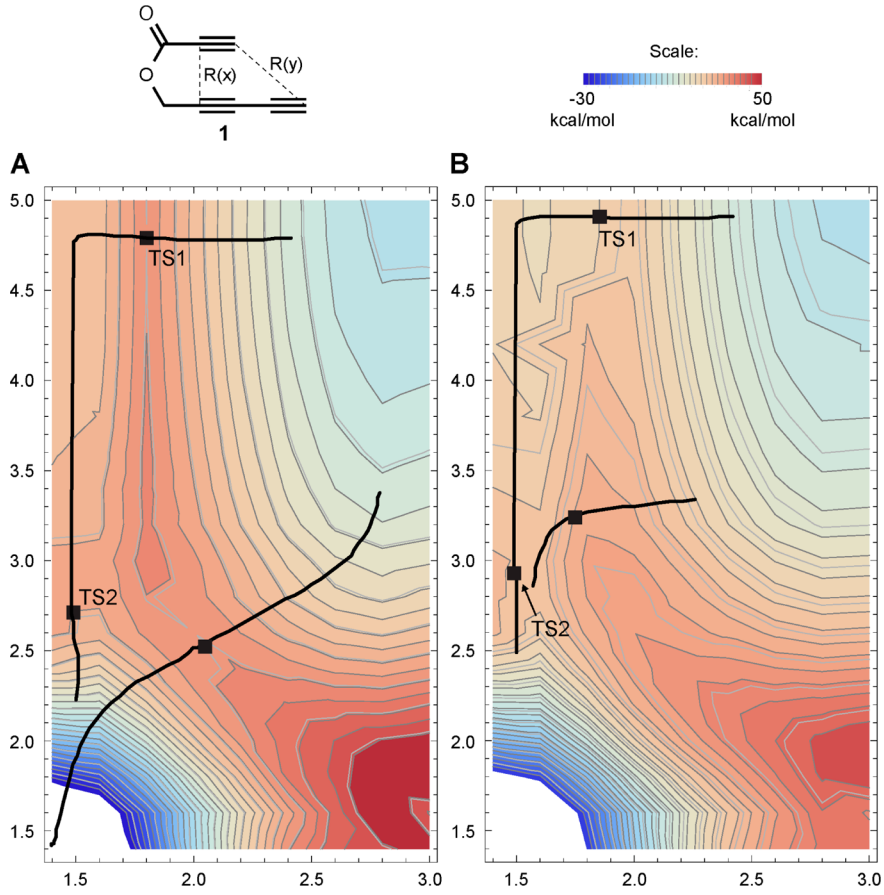

Figure 4. (A) UM06-2X/6-31+G(d,p) potential surface and (B) UB3LYP/6-31+G(d,p) potential surface for the HDDA reaction of the parent triyne **1**. Distances R(x) and R(y) are plotted on the respective x and y axes in Å. Energies in kcal/mol are relative to the optimized reactive conformer energy in each respective model chemistry. In panel A, a stepwise reaction path is illustrated proceeding from reactant, at upper right, through TS1 to an intermediate diradical, at upper left, through TS2 to products at lower left. Also shown is the path proceeding through a concerted TS. The formal concerted and stepwise reaction pathways are plotted for A and B using the default IRC algorithm in Gaussian 09. Black squares mark the location of optimized transition state geometries for each case.

DOI: 10.1021/acs.joc.5b01356
J. Org. Chem. 2015, 80, 11744−11754

the concerted TS structure were 28.9 and 36.1 kcal/mol, as predicted by the M11-L and B3LYP functionals, respectively (see SI for full details). Similarly, the smallest and largest enthalpies of activation associated with the stepwise TS structure TS1 were 22.5 and 32.4 kcal/mol, as predicted by the M11-L and M06-2X functionals, respectively. In general, functionals including higher proportions of exact (Hartree−Fock) exchange predict higher relative energies for TS structures and exhibit larger values of $\langle S^2 \rangle$ in their broken-symmetry wave functions. Above and beyond this variation associated with single-determinantal instability, there may also be some effect from the documented failure of several functionals to predict accurately the energetics of reactions in which one or more bonds are transformed from π type to σ type.[38]

Perhaps not surprisingly, given this substantial variation in relative enthalpies for fixed structures as a function of the functional, there is also substantial variation in the location of stationary points on overall cycloaddition potential energy surfaces as a function of the functional. This is illustrated in Figure 4, for instance, where the M06-2X and B3LYP levels of theory are compared using the somewhat smaller 6-31+G(d,p) basis set to map the two-dimensional surface defined by the distances between the two sets of alkyne termini. In both panels of Figure 4, two trajectories are shown. Both begin at the upper right on the reduced potential energy surface (PES), with long distances between the two sets of alkyne termini characteristic of the reactant structure. Closing the proximal C−C bond without substantially reducing the distance between the distal termini is equivalent to moving horizontally left on the PES, and that stepwise pathway proceeds through a saddle point (i.e., TS1) with a forming proximal C−C bond distance of about 1.8 Å while the distal C−C separation remains about 4.8 Å. A diradical intermediate occupies "the high plateau" at upper left in the PES, and that intermediate can continue to react by shortening the distal C−C distance, corresponding to movement vertically downward in the diagram. The trajectory passes through the saddle point TS2 (which is at lower energy than TS1) at a terminal C−C distance of about 2.9 Å and continues steeply downhill thereafter to the *o*-benzyne product at the lower left in the PES.

A second trajectory in each panel begins by reducing the terminal distance first (downward movement), followed by a coupled closure of both distances (diagonally downward left movement) until a concerted-like TS structure is reached (Figure 4), after which continued movement along the trajectory goes directly to the product. At the M06-2X/6-31+G(d,p) level of theory, the energies of TS1 and the concerted TS structure are quite close to one another. However, the generation of these surfaces is complicated by the tendency for the Kohn−Sham wave functions to exhibit restricted → unrestricted instabilities over large regions of the surface on either side of a diagonal running from upper left to lower right. Coaxing convergence to a lower energy unrestricted solution rather than a higher energy restricted solution is not always a simple task and can lead to some jaggedness in the contour plots (this is particularly evident in panel B for B3LYP).

Considering the B3LYP PES in more detail, it is apparent that on this surface there is a stepwise trajectory analogous to that on the M06-2X surface, but the concerted-like TS structure does not occur at a visible saddle point—contours to the lower right of TS1 rise monotonically in energy toward the energy peak found at the lower right in both PESs. Note that this energy peak corresponds to structures having distal bond closure preceding proximal bond closure. As was noted in the introduction, such a reaction mechanism seems intuitively unlikely, but these PES surfaces offer more quantitative support for that contention.

If we assume, for the moment, that the M06-2X TS structures are reasonably representative of saddle points for stepwise and concerted reactions on some "true" Born−Oppenheimer surface, it is worth noting that while there is substantial deviation in the absolute activation enthalpies predicted by various functionals, there is uniformity in the prediction that activation enthalpies predicted for stepwise TS1 (from broken-symmetry DFT) are always lower than those predicted for the concerted TS structure (using either a restricted or unrestricted formalism). This offers additional support for the overall mechanistic interpretation of a mechanism in which bond formation is either fully stepwise or stepwise-like. However, more convincing support requires that we consider a level of electronic structure theory that includes nondynamical electron correlation in a rigorous fashion (it is a nondynamical correlation, which is associated with near degeneracies in frontier orbital energies associated with diradicals, that causes spin symmetry breaking in the various Kohn−Sham determinants described above[18]).

Such a level of theory is second-order perturbation theory based on a complete-active space self-consistent field (CASSCF) wave function; this level is denoted CASPT2.[19] For substrate **1**, we carried out CASPT2 calculations based on a CASSCF(12,12) wave function for the same reactant, TS1, and concerted TS structures employed in our DFT calculations. We employed a triple-ζ atomic natural orbital basis set and took for the 12-electron/12-orbital active space those electrons and π and π^* orbitals associated with the three triple bonds. Results from the CASPT2 level are compared to those from the density functional models in Table 5.

Table 5. Single-Point Relative Electronic Energies (kcal/mol) for Reactant and Concerted and Stepwise TS Structures of Parent Triyne 1 at Various Levels of Theory

Structure[a]	M06-2X	B3LYP-D3BJ	CASPT2	dom. CSF wt.[b]	CAS wt.[c]
Reactant[d]	0.0	0.0	0.0	0.831	0.697
stepwise TS1	29.2	22.9	21.9	0.727	0.695
concerted TS	33.7	29.8	25.6	0.787	0.695

[a]From M06-2X-6-311+G(d,p) level of theory; see Theory/Computational Models Section. [b]Weight of the dominant configuration-state function (CSF) in the CASSCF wave function. [c]Weight of the CASSCF wave function in the PT2 expansion. [d]Structure in prereactive conformation.

CASPT2 shows good quantitative agreement with broken-symmetry B3LYP-D3BJ for the energy of stepwise TS1 relative to the reactant, while broken-symmetry M06-2X predicts a substantially higher value (consistent with its increased percentage of exact exchange compared to B3LYP, *vide supra*). CASPT2 predicts the concerted TS structure to be 3.7 kcal/mol higher in energy than TS1, which interestingly is in reasonable agreement with the separation between the two TS structures predicted by M06-2X, but is smaller than the separation predicted by B3LYP-D3BJ. Importantly, the weight of the CASSCF wave function in the PT2 expansion is

DOI: 10.1021/acs.joc.5b01356
J. Org. Chem. 2015, 80, 11744−11754

essentially identical for all three molecular structures; this suggests that the application of perturbation theory to their relative energies is not unbalanced. Also of interest, the weight of the dominant configuration-state function (in this case the restricted Hartree−Fock-like determinant) drops from 0.831, for the reactant, to 0.787, for the concerted TS structure, to 0.727, for stepwise TS1. This significant drop in the weight of the dominant configuration is entirely consistent with the tendency for the Kohn−Sham single determinants to exhibit restricted → unrestricted symmetry breaking as proximal bond formation advances along the cyclization reaction coordinate.[39]

Taken as a whole, the comparison of DFT and CASPT2 results provides additional support for a stepwise(-like) mechanism above and beyond that inferred from direct comparison of the B3LYP-D3BJ results to experiment as presented above. A single remaining vulnerability might be the theoretical reliance on geometries obtained from the M06-2X functional, in spite of that functional's generally very good performance[40] for organic geometries (for both minima and TS structures). It is not obvious, however, that any other model might be expected to offer a guaranteed improvement. Other functionals are similarly prone to symmetry breaking in the face of diradical character, and CASSCF geometries are known to be rather poor as they fail to include dynamical electron correlation during the optimization process (we have not attempted the more tedious task of CASPT2 geometry optimizations). And, while the M06-2X and B3LYP PESs in Figure 4 certainly have some qualitative differences, they are in general agreement that one would not expect a sharp drop in the energy of the concerted TS structure on the basis of small variations in otherwise roughly similar C−C bond lengths.

One remaining possibility is to consider a highly correlated post-Hartree−Fock method to provide one additional window into the computational characterization of the reaction mechanism. To that end, we investigated the CBS-QB3 composite level of theory,[22] which includes steps up to the coupled cluster level of theory including all single, double, and perturbatively estimated triple excitations. At the CBS-QB3 level (which by construction employs B3LYP optimized geometries), the concerted and stepwise TS structures are predicted to have gas-phase enthalpies of 27.4 and 29.8 kcal/mol, respectively, relative to the reactant. Thus, the CBS-QB3 level predicts the *concerted* TS structure to be lower in energy, an apparent inversion compared to all other levels. However, inspection of the T1 diagnostic[23] for the coupled cluster portion of the calculation suggests that this particular prediction is likely to be unreliable. A T1 value in excess of 0.02 for a singlet electronic state is generally taken to mean that the underlying wave function has sufficient diradical character to make the CCSD(T) model unstable.[23] The T1 values for the concerted and stepwise TS structures from our CBS-QB3 calculations, however, are 0.021 and 0.050, respectively. While the first value may be on the edge of reliability, the second considerably exceeds it (and, indeed, exceeds as well a more generous threshold of 0.044 that has been proposed as more appropriate for diradicals[41]). On that basis, we elected not to consider additional results from the CBS-QB3 model chemistry.

CONCLUSIONS

Through a comparison of theoretical models to an expanded set of experimental data and with one another, we have determined that the mechanism of the intramolecular hexadehydro-Diels−Alder proceeds in a fashion that (i) involves much more substantial bond formation between the proximal alkyne termini that are attached to the joining tether compared to bond formation between the distal alkyne termini, but that (ii) is nevertheless balanced on the knife edge of concertedness, with diradical intermediates being found to be stable on some thermodynamic surfaces but not others, depending on substitution at the distal alkyne termini. We refer to such highly asynchronous concerted pathways as "stepwise-like" insofar as diradical minima *are* in general predicted on the potential energy surface, even if they fail to remain lower in enthalpy (or free energy) than subsequent transition-state structures for completion of the cyclization once zero-point vibrational energies and thermal contributions are added to electronic energies. The modeling of these reactions is made particularly challenging because of the instability of single-determinantal models—such as Kohn−Sham density functional and Hartree−Fock theories—along key regions of the cycloaromatization reaction coordinates. Careful calibration against both experimental results and multireference wave function theories, however, permits a clear picture to emerge that supports the stepwise(-like) mechanistic assignment. Secondary kinetic isotope effects are predicted to offer another means to further distinguish between alternative mechanistic pathways, and such experiments will hopefully prove forthcoming.

EXPERIMENTAL SECTION

General Information. NMR spectra were recorded in the indicated solvent on a 500 MHz spectrometer. "The following format is used to report the proton NMR data: chemical shift in ppm [multiplicity, coupling constant(s) in Hz, integral, and assignment]. Coupling constant analysis was informed by methods we have previously reported.[42] Chemical shifts for proton spectra are referenced to TMS (δ = 0.00 ppm) for spectra recorded in $CDCl_3$. Nonfirst-order multiplets are identified as 'nfom'."[43] Chemical shifts for ^{13}C NMR spectra are referenced to $CDCl_3$ (δ = 77.16 ppm). "Infrared spectral data were collected on an FT-IR spectrometer. Spectra were collected as thin films in attenuated total reflectance (ATR) mode on a germanium window."[43] HRMS data were obtained using an electrospray ionization (ESI) mass spectrometer. Samples were doped with either PPG or PEG as an internal calibrant and then were introduced as a methanolic solution. "MPLC (medium pressure liquid chromatography) was performed at 25−200 psi. Columns were hand-packed with silica gel (18−32 μm, 60 Å pore size)."[43] An HPLC pump outfitted with a differential refractive index detector was used. Flash chromatography was performed on silica gel. "Thin layer chromatography was carried out on glass or plastic backed plates of silica gel. Spots were visualized by UV irradiation and/or dipping in a solution of anisaldehyde, phosphomolybdic acid, potassium permanganate, or ceric ammonium molybdate followed by heat treatment. Reactions requiring anhydrous conditions were performed in flame- or oven-dried glassware under an inert atmosphere (nitrogen or argon). Anhydrous diethyl ether, toluene, THF, and methylene chloride were passed through a column of activated alumina and tapped immediately prior to use. $CHCl_3$ used as a medium for the HDDA reaction was ethanol-free. Reported (external) reaction temperatures are the temperature of the heating bath. HDDA initiated reactions, including those that were carried out at temperatures above the boiling point of the solvent, were typically carried out in a screw-capped vial or culture tube fitted with an inert, Teflon-lined cap."[43]

Procedure for Determination of HDDA Half-Lives. A 0.1 M solution of the HDDA polyyne substrate in *o*-DCB was prepared and AcOH (10−50 equiv) was added. The vial was sealed with a Teflon-lined cap, and the solution was placed in a silicone oil bath that had been pre-equilibrated to a desired temperature. At various time points, an aliquot (ca. 15 μL) was diluted in $CDCl_3$ (600 μL) and analyzed

DOI: 10.1021/acs.joc.5b01356
J. Org. Chem. 2015, 80, 11744−11754

directly via ^{1}H NMR spectroscopy (500 MHz, nt = 32). Peak integration of a resonance in the starting material vs the ^{13}C satellite resonance for the *o*-DCB was used to judge the extent of starting material consumption. Rate constants (k) were determined from the experimentally measured half-lives of HDDA substrates assuming unimolecular first-order kinetics. An Arrhenius pre-exponential factor (A) of 8.78×10^8 s^{-1} was previously determined from the temperature-dependence of the rate via an Arrhenius plot for the analog of ester **1** having R^1 = TMS and R^2 = $(CH_2)_2$OTBS.[43] Activation energies E_a were calculated from the Arrhenius equation ($k = Ae^{-E_a/RT}$) based on single-temperature measurements using this same value of A for all substrates reported here having free rotation about all single bonds in the tethering fragment. By contrast, an Arrhenius pre-exponential factor (A) of 1.42×10^{10} s^{-1} was previously determined from the temperature-dependence of the rate via an Arrhenius plot for the analog of ester **1** having R^1 = TMS and R^2 = $(CH_2)_2$OTBS but with the O−CH_2 ester linkage fragment replaced by a benzene ring (compound **16**).[43] Activation energies for substrates having similarly restricted rotation about this tether linkage (compounds **13**, **16**, and **18**) were calculated from single-temperature measurements via the Arrhenius equation using this A value. For comparison to theory, enthalpies of activation were determined according to the relationship $E_a = \Delta H^{\ddagger} + RT$.[18]

Preparation procedures and characterization data for 2−6 and 8−12, which are all of the compounds newly described in this report.

5-(Trimethylsilyl)penta-2,4-diyn-1-yl propiolate (2). A solution of 5-(trimethylsilyl)penta-2,4-diyn-1-ol[44] (230 mg, 1.5 mmol) and propiolic acid (110 μL, 1.8 mmol) in dichloromethane (10 mL) was cooled to 0 °C. *N,N′*-Dicyclohexylcarbodiimide (370 mg, 1.8 mmol) and DMAP (15 mg, 0.12 mmol) were added, and the mixture was allowed to come to room temperature. After 4 h the solution was filtered through a plug of Celite, rinsing with EtOAc. After solvent removal the crude material was purified by MPLC (15:1 Hex/EtOAc) to give triyne **2** (155 mg, 0.76 mmol, 51%) as an amber oil. ^{1}H NMR (500 MHz, $CDCl_3$): δ 4.84 (s, 2H), 2.96 (s, 1H), and 0.20 (s, 9H). ^{13}C NMR (125 MHz, $CDCl_3$): δ 151.7, 89.1, 86.7, 76.3, 73.8, 72.5, 69.9, 53.9, and −0.5. IR: 3291, 2963, 2123, 1724, 1252, 1207, 966, 848, and 753 cm^{-1}. HR ESI-MS calcd for $C_{11}H_{12}NaO_2Si$ [M + Na]$^+$ 227.0499, found 227.0482.

5-(*tert*-Butyldimethylsilyl)penta-2,4-diyn-1-yl Propiolate (3). A solution of 5-(*tert*-butyldimethylsilyl)penta-2,4-diyn-1-ol[45] (194 mg, 1.0 mmol) and propiolic acid (75 μL, 1.2 mmol) in dichloromethane (8 mL) was cooled to 0 °C. *N,N′*-Dicyclohexylcarbodiimide (247 mg, 1.2 mmol) and DMAP (15 mg, 0.12 mmol) were added and the mixture was allowed to come to room temperature. After 2 h the solution was filtered through a plug of Celite, rinsing with EtOAc. After solvent removal the crude material was purified by MPLC (10:1 Hex:EtOAc) to give triyne **3** (168 mg, 0.68 mmol, 68%) as an amber oil. ^{1}H NMR (500 MHz, $CDCl_3$): δ 4.85 (s, 2H), 2.96 (s, 1H), 0.94 (s, 9H), and 0.14 (s, 6H). ^{13}C NMR (125 MHz, $CDCl_3$): δ 151.8, 87.9, 87.4, 76.3, 73.9, 72.7, 69.4, 54.0, 26.1, 16.8, and −4.8. IR: 3290, 2954, 2931, 2858, 2123, 1725, 1208, 830, and 778 cm^{-1}. HR ESI-MS calcd for $C_{14}H_{18}NaO_2Si$ [M + Na]$^+$ 269.0972, found 269.0957.

5-(Triphenylsilyl)penta-2,4-diyn-1-yl Propiolate (4). 5-(Triphenylsilyl)penta-2,4-diyn-1-ol was prepared as follows: Under an inert atmosphere, triphenylsilyl acetylene (284 mg, 1.0 mmol) and 3-bromopropargyl alcohol (335 mg, 2.5 mmol) were dissolved in 4 mL of freshly deaerated piperidine, and the solution was cooled to 0 °C. CuCl (40 mg, 0.4 mmol) was added, and the reaction mixture was stirred for 1.5 h at 0 °C. The mixture was diluted with satd aq. NH_4Cl and extracted with EtOAc. The combined organic extracts were washed with brine, dried ($MgSO_4$), and concentrated. Purification by MPLC (3:1 Hex/EtOAc) gave 5-(triphenylsilyl)penta-2,4-diyn-1-ol (125 mg, 0.40 mmol, 40%) as a clear oil {^{1}H NMR (500 MHz, $CDCl_3$): δ 7.63 [dt, J = 6.6, 1.4 Hz, 6H], 7.45 [tt, J = 7.4, 1.4 Hz, 3H], 7.39 [ddd, J = 7.5, 6.7, and 1.4 Hz, 6H], 4.37 (s, 2H), and 1.64 (br s, 1H)}. A solution of this 5-(triphenylsilyl)penta-2,4-diyn-1-ol (110 mg, 0.32 mmol) and propiolic acid (30 μL, 0.48 mmol) in dichloromethane (3 mL) was cooled to 0 °C. *N,N′*-Dicyclohexylcarbodiimide (100 mg, 0.48 mmol) and DMAP (5 mg, 0.04 mmol) were added, and the mixture was allowed to come to room temperature. After 4 h the solution was filtered through a plug of Celite, rinsing with EtOAc. After solvent removal the crude material was purified by MPLC (12:1 Hex/EtOAc) to give triyne **4** (65 mg, 0.17 mmol, 51%) as a clear oil. ^{1}H NMR (500 MHz, $CDCl_3$): δ 7.62 (dd, J = 8.0, 1.4 Hz, 6H), 7.45 (ddd, J = 7.3, 7.3, 1.4 Hz, 3H), 7.39 (ddd, J = 7.5, 6.8, 1.4 Hz, 6H), 4.86 (s, 2H), and 2.95 (s, 1H). ^{13}C NMR (125 MHz, $CDCl_3$): δ 151.7, 135.7, 132.2, 130.4, 128.3, 90.7, 84.0, 76.5, 73.8, 72.6, 71.3, and 53.9. IR: 3272, 3069, 3050, 3023, 2119, 1724, 1429, 1208, 1113, 967, 806, and 749 cm^{-1}. HR ESI-MS calcd for $C_{26}H_{18}NaO_2Si$ [M + Na]$^+$ 413.0968, found 413.0979.

Penta-2,4-diyn-1-yl 3-(trimethylsilyl)propiolate (5). A solution of penta-2,4-diyn-1-ol[46](60 mg, 0.75 mmol) and 3-trimethylsilylpropynoic acid (140 mg, 1.0 mmol) in dichloromethane (7 mL) was cooled to 0 °C. *N,N′*-Dicyclohexylcarbodiimide (206 mg, 1.0 mmol) and DMAP (10 mg, 0.08 mmol) were added, and the mixture was allowed to come to room temperature. After 4 h the solution was filtered through a plug of Celite, rinsing with EtOAc. After solvent removal the crude material was purified by MPLC (20:1 Hex/EtOAc) to give triyne **5** (65 mg, 0.32 mmol, 42%) as an amber oil. ^{1}H NMR (500 MHz, $CDCl_3$): δ 4.81 (s, 2H), 2.23 (s, 1H), and 0.26 (s, 9H). ^{13}C NMR (125 MHz, $CDCl_3$): δ 151.9, 96.3, 93.4, 71.6, 69.3, 69.1, 67.1, 53.4, and −0.8. IR: 3294, 2965, 2363, 2344, 2175, 2118 1719, 1253, 1205, 848, and 760 cm^{-1}. HR ESI-MS calcd for $C_{11}H_{12}NaO_2Si$ [M + Na]$^+$ 227.0499, found 227.0489.

5-(Trimethylsilyl)penta-2,4-diyn-1-yl 3-(trimethylsilyl)-propiolate (6). The following reagents were added in sequence to CH_2Cl_2 (5 mL) at 0 °C: 5-(trimethylsilyl)penta-2,4-diyn-1-ol (137 mg, 0.9 mmol), 3-trimethylsilylpropynoic acid (142 mg, 1.0 mmol), EDCI (170 mg, 1.1 mmol), and DMAP (12 mg, 0.1 mmol). The resulting homogeneous solution quickly became cloudy. After 3 h the suspension was diluted with H_2O and extracted with CH_2Cl_2. The combined organic extracts were washed with brine, dried ($MgSO_4$), and concentrated. Purification by MPLC (10:1 hexanes/EtOAc) gave the ester **6** (140 mg, 0.51 mmol, 51%) as a clear oil. ^{1}H NMR (500 MHz, $CDCl_3$): δ 4.81 (s, 2H), 0.25 (s, 9H), and 0.20 (s, 9H). ^{13}C NMR (125 MHz, $CDCl_3$): δ 152.0, 96.2, 93.5, 88.9, 86.8, 72.3, 70.3, 53.6, −0.4, and −0.8. IR: 2965, 2903, 2114, 1721, 1253, 1205, 851, and 760 cm^{-1}. HR ESI-MS calcd for $C_{14}H_{20}NaO_2Si_2$ [M + Na]$^+$ 299.0894, found 299.0898.

1-Oxo-6-(trimethylsilyl)-1,3-dihydroisobenzofuran-5-yl acetate (8). A solution of triyne **2** (24 mg, 0.12 mmol) and acetic acid (70 μL, 10 equiv) in DCB (1.0 mL) was heated at 120 °C. After 24 h the solution was loaded onto a column of silica and DCB was removed by initial elution with hexanes. Subsequent elution with hexanes/EtOAc (2:1) gave the benzenoid **8** (28 mg, 0.11 mmol, 90%) as a yellow oil. ^{1}H NMR (500 MHz, $CDCl_3$): δ 8.05 (d, J = 0.6 Hz, 1H), 7.27 (t, J = 0.8 Hz, 1H), 5.30 (d, J = 1.2 Hz, 2H), 2.37 (s, 3H), and 0.33 (s, 9H). ^{13}C NMR (125 MHz, $CDCl_3$): δ 170.5, 168.8, 159.7, 149.2, 134.2, 133.2, 122.8, 115.8, 69.2, 21.6, and −1.0. IR (neat): 2954, 2900, 1762, 1618, 1248, 1190, 1136, 1068, 1010, and 843 cm^{-1}. HRMS (ESI-TOF): Calcd for $C_{13}H_{16}NaO_4Si^+$ [M+H$^+$] requires 287.0710; found 287.0721.

6-(*tert*-Butyldimethylsilyl)-1-oxo-1,3-dihydroisobenzofuran-5-yl acetate (9). A solution of triyne **3** (35 mg, 0.14 mmol) and acetic acid (80 μL, 10 equiv) in DCB (1.4 mL) was heated at 135 °C. After 18 h the solution was loaded onto a column of silica and DCB was removed by initial elution with hexanes. Subsequent elution with hexanes/EtOAc (2:1) gave benzenoid **9** (33 mg, 0.11 mmol, 76%) as a yellow oil. ^{1}H NMR (500 MHz, $CDCl_3$): δ 8.05 (s, 1H), 7.28 (t, J = 0.8 Hz, 1H), 5.31 (d, J = 0.9 Hz, 2H), 2.36 (s, 3H), 0.90 (s, 9H) and 0.35 (s, 6H). ^{13}C NMR (125 MHz, $CDCl_3$): δ 170.6, 168.9, 159.7, 149.0, 134.5, 131.7, 122.6, 116.1, 69.2, 60.6, 53.6, 26.7, 21.8, 17.6, and −4.7. IR (neat): 2953, 2930, 2883, 2857, 1764, 1618, 1250, 1189, 1065, 1010, 837, and 768 cm^{-1}. HRMS (ESI-TOF): Calcd for $C_{16}H_{22}NaO_4Si^+$ [M+Na$^+$] requires 329.1180; found 329.1182.

6-(Triphenylsilyl)-1-oxo-1,3-dihydroisobenzofuran-5-yl acetate (10). A solution of triyne **4** (20 mg, 0.05 mmol) and acetic acid (30 μL, 10 equiv) in DCB (0.5 mL) was heated at 135 °C. After 24 h the solution was loaded onto a column of silica and DCB was removed

DOI: 10.1021/acs.joc.5b01356
J. Org. Chem. 2015, 80, 11744−11754

by initial elution with hexanes. Subsequent elution with hexanes/EtOAc (2:1) gave benzenoid **10** (22 mg, 0.05 mmol, 95%) as a yellow oil containing minor impurities. ^{1}H NMR (500 MHz, $CDCl_3$): δ 7.91 (d, J = 0.5 Hz, 1H), 7.54 (dd, J = 8.0, 1.4 Hz, 6H), 7.46 (tt, J = 7.4, 1.5 Hz, 3H), 7.40 (m, 6H), 7.37 (t, J = 1.4 Hz, 1H), 5.34 (d, J = 1.3 Hz, 2H), and 1.38 (s, 3H). ^{13}C NMR (125 MHz, $CDCl_3$): δ 170.2, 168.3, 159.8, 150.3, 136.5, 136.1, 132.8, 130.2, 129.4, 128.3, 122.9, 116.6, 69.2, and 20.2. IR (neat): 2955, 2922, 1767, 1618, 1457, 1429, 1371, 1293, 1247, 1185, 1136, 1109, 1067, and 1012 cm^{-1}. GC-MS t_r (5031022) = 15.37 min; m/z: 373, 331, 253, 207. HRMS: (ESI-TOF): Calcd for $C_{28}H_{22}NaO_4Si^+$ [M+Na$^+$] requires 473.1180; found 473.1187.

1-Oxo-7-(trimethylsilyl)-1,3-dihydroisobenzofuran-5-yl acetate (11). A solution of triyne **5** (20 mg, 0.10 mmol) and acetic acid (110 μL, 20 equiv) in DCB (9.0 mL) was heated at 125 °C. After 24 h the solution was loaded onto a column of silica and DCB was removed by initial elution with hexanes. Subsequent elution with hexanes/EtOAc (2:1) gave the crude product. Purification via MPLC (5:1 Hex/EtOAc) gave benzenoid **11** (24 mg, 0.09 mmol, 93%) as a yellow oil. ^{1}H NMR (500 MHz, $CDCl_3$): δ 7.31 (d, J = 2.0 Hz, 1H), 7.23 (dt, J = 1.9, 0.9 Hz, 1H), 5.29 (d, J = 0.7 Hz, 2H), 2.36 (s, 3H), and 0.40 (s, 9H). ^{13}C NMR (125 MHz, $CDCl_3$): δ 170.9, 169.1, 154.2, 148.6, 144.4, 128.8, 127.5, 115.9, 69.0, 21.3, and −1.2. IR (neat): 2934, 2855, 1759, 1588, 1194, 1128, 1048, 1010, 843, and 757 cm^{-1}. HRMS (ESI-TOF): Calcd for $C_{13}H_{16}NaO_4Si^+$ [M+H$^+$] requires 287.0710; found 287.0705.

1-Oxo-6-(trimethylsilyl)-1,3-dihydroisobenzofuran-5-yl acetate (12). A solution of triyne **6** (27 mg, 0.10 mmol) and acetic acid (60 μL, 10 equiv) in DCB (1.0 mL) was heated at 120 °C. After 24 h the solution was loaded onto a column of silica and DCB was removed by initial elution with hexanes. Subsequent elution with hexanes/EtOAc (5:1) gave the benzenoid **12** (28 mg, 0.08 mmol, 85%) as a yellow oil. ^{1}H NMR (500 MHz, $CDCl_3$): δ 7.16 (t, J = 0.7 Hz, 1H), 5.24 (d, J = 0.8 Hz, 2H), 2.36 (s, 3H), 0.44 (s, 9H), and 0.39 (s, 9H). ^{13}C NMR (125 MHz, $CDCl_3$): δ 171.1, 169.0, 159.2, 155.3, 148.1, 143.0, 129.3, 115.0, 68.6, 21.9, and 2.7 (2). IR (neat): 2952, 2902, 1760, 1249, 1190, 1141, 1058, 1017, 844, and 757 cm^{-1}. HRMS (ESI-TOF): Calcd for $C_{16}H_{24}NaO_4Si_2^+$ [M+H$^+$] requires 359.1105; found 359.1113.

■ ASSOCIATED CONTENT

Supporting Information

The Supporting Information is available free of charge on the ACS Publications website at DOI: 10.1021/acs.joc.5b01356.

Cartesian coordinates and electronic energies for all stationary points, as well as energetics comparisons using different density functionals. Listing of ^{1}H NMR data with authors' assignments of resonances with their associated protons. Copies of ^{1}H and ^{13}C NMR spectra of all newly reported compounds (PDF)

■ AUTHOR INFORMATION

Corresponding Authors

*E-mail: cramer@umn.edu.
*E-mail: hoye@umn.edu.
*E-mail: kuwata@macalester.edu.

Author Contributions

§D.J.M. and L.R.F. contributed equally.

Notes

The authors declare no competing financial interest.

■ ACKNOWLEDGMENTS

This investigation was supported by grants awarded by the U.S. Department of Health and Human Services (National Institute of General Medical Sciences, GM-65597) and the U.S. National Science Foundation (CHE-1361595 and CHE-1039925, the latter a Major Research Instrumentation grant to the Midwest Undergraduate Computational Chemistry Consortium). Some of the computational aspects of this work were performed with software and hardware software made available through the University of Minnesota Supercomputing Institute (MSI). NMR spectra were recorded on an instrument purchased with support from the NIH Shared Instrumentation Grant program (S10OD011952). We thank Vedamayee Pogula and Moriana Haj for performing several repeat experiments and Professor Laura Gagliardi for having carried out the CASPT2(12,12) calculations.

■ REFERENCES

(1) Bradley, A. Z.; Johnson, R. P. *J. Am. Chem. Soc.* **1997**, *119*, 9917−9918.
(2) Miyawaki, K.; Suzuki, R.; Kawano, T.; Ueda, I. *Tetrahedron Lett.* **1997**, *38*, 3943−3946.
(3) Holden, C.; Greaney, M. F. *Angew. Chem., Int. Ed.* **2014**, *53*, 5746−5749.
(4) Hoye, T. R.; Baire, B.; Niu, D. W.; Willoughby, P. H.; Woods, B. P. *Nature* **2012**, *490*, 208−212.
(5) Yun, S. Y.; Wang, K.-P.; Lee, N.-K.; Mamidipalli, P.; Lee, D. *J. Am. Chem. Soc.* **2013**, *135*, 4668−4671.
(6) Niu, D.; Willoughby, P. H.; Woods, B. P.; Baire, B.; Hoye, T. R. *Nature* **2013**, *501*, 531−534.
(7) Ajaz, A.; Bradley, A. Z.; Burrell, R. C.; Li, W. H. H.; Daoust, K. J.; Bovee, L. B.; DiRico, K. J.; Johnson, R. P. *J. Org. Chem.* **2011**, *76*, 9320−9328.
(8) Liang, Y.; Hong, X.; Yu, P.; Houk, K. N. *Org. Lett.* **2014**, *16*, 5702−5705.
(9) Kerisit, N.; Toupet, L.; Larini, P.; Perrin, L.; Guillemin, J.-C.; Trolez, Y. *Chem. - Eur. J.* **2015**, *21*, 6042−6047.
(10) Zhao, Y.; Truhlar, D. G. *Theor. Chem. Acc.* **2008**, *120*, 215−241.
(11) Hehre, W. J.; Radom, L.; Schleyer, P. v. R.; Pople, J. A. *Ab Initio Molecular Orbital Theory*; Wiley: New York, 1986.
(12) Zhao, Y.; Truhlar, D. G. *Chem. Phys. Lett.* **2011**, *502*, 1−13.
(13) (a) Becke, A. D. *Phys. Rev. A: At., Mol., Opt. Phys.* **1988**, *38*, 3098−3100. (b) Lee, C.; Yang, W.; Parr, R. G. *Phys. Rev. B: Condens. Matter Mater. Phys.* **1988**, *37*, 785−789. (c) Becke, A. D. *J. Chem. Phys.* **1993**, *98*, 5648−5652. (d) Stephens, P. J.; Devlin, F. J.; Chabalowski, C. F.; Frisch, M. J. *J. Phys. Chem.* **1994**, *98*, 11623−11627.
(14) Grimme, S.; Antony, J.; Ehrlich, S.; Krieg, H. *J. Chem. Phys.* **2010**, *132*, 154104.
(15) Johnson, E. R.; Becke, A. D. *J. Chem. Phys.* **2006**, *124*, 174104.
(16) Marenich, A. V.; Cramer, C. J.; Truhlar, D. G. *J. Phys. Chem. B* **2009**, *113*, 6378−6396.
(17) Yamaguchi, K.; Jensen, F.; Dorigo, A.; Houk, K. N. *Chem. Phys. Lett.* **1988**, *149*, 537−542.
(18) Cramer, C. J. *Essentials of Computational Chemistry: Theories and Models*, 2nd ed.; John Wiley & Sons: Chichester, U.K., 2004.
(19) (a) Andersson, K.; Malmqvist, P.-Å.; Roos, B. O.; Sadlej, A. J.; Wolinski, K. *J. Phys. Chem.* **1990**, *94*, 5483−5488. (b) Andersson, K.; Malmqvist, P.-Å.; Roos, B. O. *J. Chem. Phys.* **1992**, *96*, 1218−1226.
(20) Roos, B. O.; Lindh, R.; Malmqvist, P.-Å.; Veryazov, V.; Widmark, P.-O. *J. Phys. Chem. A* **2004**, *108*, 2851−2858.
(21) Ghigo, G.; Roos, B. O.; Malmqvist, P.-Å. *Chem. Phys. Lett.* **2004**, *396*, 142.
(22) Montgomery, J. A.; Frisch, M. J.; Ochterski, J. W.; Petersson, G. A. *J. Chem. Phys.* **1999**, *110*, 2822−2827.
(23) Lee, T. J.; Taylor, P. R. *Int. J. Quantum Chem.* **1989**, *36*, 199−207.
(24) The stabilizing effect of α-silyl substitution has been discussed in the literature, with both electronic and rehybridization effects being suggested to be important. (a) Laub, H. A.; Mayr, H. *Chem. - Eur. J.* **2014**, *20*, 1103−1110. (b) Alabugin, I. V.; Bresch, S.; Manoharan, M. *J. Phys. Chem. A* **2014**, *118*, 3663−3677.

DOI: 10.1021/acs.joc.5b01356
J. Org. Chem. 2015, 80, 11744−11754

(25) Woods, B. P.; Baire, B.; Hoye, T. R. *Org. Lett.* **2014**, *16*, 4578−4581.
(26) (a) Mayer, J.; Sondheimer, F. *J. Am. Chem. Soc.* **1966**, *88*, 602−603. (b) Gleiter, R.; Ritter, J. *Angew. Chem., Int. Ed. Engl.* **1995**, *33*, 2470−2472. (c) Haberhauer, G.; Gleiter, R. *J. Am. Chem. Soc.* **1999**, *121*, 4664−4668.
(27) Haberhauer, G.; Gleiter, R.; Fabig, S. *Org. Lett.* **2015**, *17*, 1425−1428.
(28) (a) Maretina, I. A.; Trofimov, B. A. *Russ. Chem. Rev.* **2000**, *69*, 591−608. (b) Glen, A. T.; Hutchinson, S. A.; McCorkindale, N. J. *Tetrahedron Lett.* **1966**, *7*, 4223−4225.
(29) (a) Cramer, C. J.; Nash, J. J.; Squires, R. R. *Chem. Phys. Lett.* **1997**, *277*, 311−320. (b) Debbert, S. L.; Cramer, C. J. *Int. J. Mass Spectrom.* **2000**, *201*, 1−15. (c) de Visser, S. P.; Filatov, M.; Shaik, S. *Phys. Chem. Chem. Phys.* **2000**, *2*, 5046−5048.
(30) Pellissier, H.; Santelli, M. *Tetrahedron* **2003**, *59*, 701−730.
(31) (a) Jones, R. R.; Bergman, R. G. *J. Am. Chem. Soc.* **1972**, *94*, 660. (b) Bergman, R. G. *Acc. Chem. Res.* **1973**, *6*, 25−31.
(32) (a) Kraka, E.; Cremer, D. *J. Am. Chem. Soc.* **1994**, *116*, 4929−4936. (b) Cramer, C. J. *J. Am. Chem. Soc.* **1998**, *120*, 6261−6269. (c) Schreiner, P. R. *Chem. Commun.* **1998**, 483−484. (d) Mohamed, R. K.; Peterson, P. W.; Alabugin, I. V. *Chem. Rev.* **2013**, *113*, 7089−7129. (e) Kraka, E.; Cremer, D. *Wiley Interdisciplinary Reviews-Computational Molecular Science* **2014**, *4*, 285−324.
(33) (a) Myers, A. G. *Tetrahedron Lett.* **1987**, *28*, 4493−4496. (b) Nagata, R.; Yamanaka, H.; Okazaki, E.; Saito, I. *Tetrahedron Lett.* **1989**, *30*, 4995−4998.
(34) Schmittel, M.; Strittmatter, M.; Kiau, S. *Tetrahedron Lett.* **1995**, *36*, 4975−4978.
(35) (a) Schreiner, P. R.; Prall, M. *J. Am. Chem. Soc.* **1999**, *121*, 8615−8627. (b) Cramer, C. J.; Kormos, B. L.; Seierstad, M.; Sherer, E. C.; Winget, P. *Org. Lett.* **2001**, *3*, 1881−1884. (c) de Visser, S. P.; Filatov, M.; Shaik, S. *Phys. Chem. Chem. Phys.* **2001**, *3*, 1242−1245. (d) Schmittel, M.; Steffen, J. P.; Maywald, M.; Engels, B.; Helten, H.; Musch, P. *J. Chem. Soc., Perkin Trans. 2* **2001**, 1331−1339.
(36) Cramer, C. J.; Squires, R. R. *Org. Lett.* **1999**, *1*, 215−218.
(37) (a) Dewar, M. J. S. *J. Am. Chem. Soc.* **1984**, *106*, 209−219. (b) Borden, W. T.; Loncharich, R. J.; Houk, K. N. *Annu. Rev. Phys. Chem.* **1988**, *39*, 213−236. (c) Houk, K. N.; Gonzalez, J.; Li, Y. *Acc. Chem. Res.* **1995**, *28*, 81−90.
(38) Pieniazek, S. N.; Clemente, F. R.; Houk, K. N. *Angew. Chem., Int. Ed.* **2008**, *47*, 7746−7749.
(39) Schmidt, M. W.; Gordon, M. S. *Annu. Rev. Phys. Chem.* **1998**, *49*, 233−266.
(40) Zhao, Y.; Truhlar, D. G. *Acc. Chem. Res.* **2008**, *41*, 157−167.
(41) Rienstra-Kiracofe, J. C.; Allen, W. D.; Schaefer, H. F. *J. Phys. Chem. A* **2000**, *104*, 9823−9840.
(42) (a) Hoye, T. R.; Hanson, P. R.; Vyvyan, J. R. *J. Org. Chem.* **1994**, *59*, 4096−4103. (b) Hoye, T. R.; Zhao, H. *J. Org. Chem.* **2002**, *67*, 4014−4016.
(43) From Supporting Information for: Niu, D.; Wang, T.; Woods, B. P.; Hoye, T. R. *Org. Lett.* **2014**, *16*, 254−257.
(44) Bowling, N. P.; Burrmann, N. J.; Halter, R. J.; Hodges, J. A.; McMahon, R. J. *J. Org. Chem.* **2010**, *75*, 6382−6390.
(45) Marino, J. P.; Nguyen, H. N. *J. Org. Chem.* **2002**, *67*, 6841−6844.
(46) Turlington, M.; Du, Y.; Ostrum, S. G.; Santosh, V.; Wren, K.; Lin, T.; Sabat, M.; Pu, L. *J. Am. Chem. Soc.* **2011**, *133*, 11780−11794.

■ NOTE ADDED AFTER ASAP PUBLICATION

This paper was published ASAP on August 25, 2015. Reference 9 was added. The revised paper was reposted on October 14, 2015.

DOI: 10.1021/acs.joc.5b01356
J. Org. Chem. 2015, 80, 11744−11754